

Ultra-thin plasmonic optical vortex plate based on phase discontinuities

Patrice Genevet,^{1,2} Nanfang Yu,¹ Francesco Aieta,^{1,3} Jiao Lin,^{1,4} Mikhail A. Kats,¹ Romain Blanchard,¹ Marlan O. Scully,² Zeno Gaburro,^{1,5} and Federico Capasso^{1,a)}

¹*School of Engineering and Applied Sciences, Harvard University, Cambridge, Massachusetts 02138, USA*

²*Institute for Quantum Studies and Department of Physics, Texas A&M University, College Station, Texas 77843, USA*

³*Dipartimento di Fisica e Ingegneria dei Materiali e del Territorio, Università Politecnica delle Marche, 60131 Ancona, Italy*

⁴*Singapore Institute of Manufacturing Technology, Singapore 638075, Singapore*

⁵*Dipartimento di Fisica, Università degli Studi di Trento, 14, 38100 Trento, Italy*

(Received 19 October 2011; accepted 9 November 2011; published online 3 January 2012)

A flat optical device that generates optical vortices with a variety of topological charges is demonstrated. This device spatially modulates light beams over a distance much smaller than the wavelength in the direction of propagation by means of an array of V-shaped plasmonic antennas with sub-wavelength separation. Optical vortices are shown to develop after a sub-wavelength propagation distance from the array, a feature that has major potential implications for integrated optics. © 2012 American Institute of Physics. [doi:10.1063/1.3673334]

Traditional optical components that control the wavefront of light beams rely on the phase accumulated while light propagates in materials.¹ This concept has been extensively used to create a variety of optical components such as lenses, prisms, gratings, and spiral phase plates. Spatial light modulators (SLMs) are the most sophisticated devices based on this mechanism and have found numerous applications ranging from displays and projectors to holographic optical tweezers.^{2,3} SLMs are based on the local control of the orientation of anisotropic liquid crystal molecules, which creates a spatially varying distribution of the index of refraction. A light beam propagating through liquid crystal cells containing molecules with different orientations will experience spatially varying phase velocity, resulting in transverse modulation of either its phase and/or its amplitude.

Recently, a method to control the phase and amplitude of light beams was demonstrated by using the concept of phase discontinuities, which has led to a generalization of the laws of reflection and refraction.⁴ Preliminary results on the generation of single-charge optical vortices were also shown. In this paper we perform a detailed experimental and theoretical study of single- and double-charged vortices and demonstrate that their phase profile is controlled over a sub-wavelength propagation distance. Using the concept of phase discontinuities, we have achieved independent control of the phase and the amplitude for a state of polarization orthogonal to the incident polarization. Our experiments, in excellent agreement with simulations, show that optical vortices with different orbital angular momentum^{5,6} can be created when conventional Gaussian beams traverse an interface that imprints a screw-like phase profile on the incident beam.

Optical vortices are a peculiar type of beam that has a doughnut-like intensity profile and an azimuthal phase dependence ($\exp(i\ell\theta)$) with respect to the beam axis (that is a helicoidally shaped wavefront). The number of twists (ℓ) of the wavefront within a wavelength is called the topological

charge of the vortex beam and is related to the orbital angular momentum L of photons by the relationship $L = \hbar\ell$, where \hbar is the Planck constant.⁷ Optical beams with such helical phase profile are conventionally generated using spiral phase plates,⁸ spatial light modulators,⁹ or holograms.¹⁰ This type of beam can also be directly generated by lasers as an intrinsic transverse mode¹¹ or when an incident beam diffracts from fork-shaped intensity masks.¹⁰ Optical vortices are of great fundamental interest since they carry optical singularities^{5,12} and can attract and annihilate each other in pairs, making them the optical analogue of superfluid vortices.^{13,14} Vortex beams are also important for a number of applications such as stimulated emission depletion microscopy,¹⁵ optical trapping,³ and in optical communication systems, where the spiral phase can carry additional information.^{16,17}

Fig. 1 shows the experimental setup used to generate and characterize the optical vortices. It consists of a Mach-Zehnder interferometer where the optical vortices are generated in one arm and their optical wavefronts are revealed by interference with a reference Gaussian beam propagating through the other arm. A laser beam from a distributed feedback quantum cascade laser (DFB-QCL) operating at $\lambda = 7.75 \mu\text{m}$ in continuous wave mode with power of ~ 10 mW is collimated and separated in two parts by a beam splitter. One part of the beam is rotated in polarization using a set of mirrors and expanded to serve as a reference beam. The second part is focused on the thin phase plate using a ZnSe lens (20-in. focal length, 1-in. diameter). The phase plate comprises a silicon interface patterned with a 2D arrangement of V-shaped gold plasmonic antennas designed and placed so that the cross-polarized scattered light from the modulator forms an optical vortex. As described in detail in Ref. 4, any optical element with a sub-wavelength size in the propagation direction that can “trap and release” the electromagnetic field with a controllable phase shift can be a good candidate for creating phase discontinuities. In the experiments reported in Ref. 4 and in the present work, the resonators are optical antennas designed to have the same scattering cross section but a controllable phase shift ranging

^{a)} Author to whom correspondence should be addressed. Electronic mail: capasso@seas.harvard.edu.

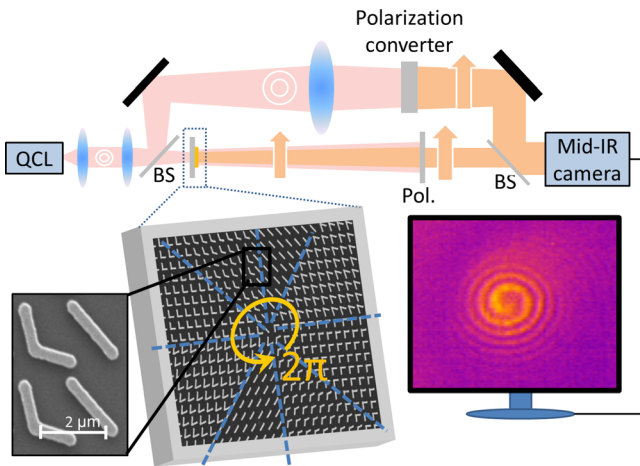


FIG. 1. (Color online) Experimental setup. A normally incident S-polarized beam from a quantum cascade laser emitting at $\lambda = 7.75 \mu\text{m}$ is separated into two beams by a beam splitter. The first beam is focused onto the interface, which is patterned with an azimuthal distribution of eight types of plasmonic antennas with sub-wavelength separations compared to the free space wavelength (λ). The interface generates a cross polarized beam with a screw-like phase profile. The P-polarized scattered light, in the form of a vortex beam, is then filtered using a polarizer and is combined with the reference beam propagating through the second arm of a Mach-Zehnder interferometer. The reference beam is rotated in polarization (90°) using a set of mirrors. The interference between the vortex beam and the reference Gaussian beam is recorded using a mid-infrared camera. After the beam splitter, the Gaussian and vortex beams are parallel and spatially overlapped. The intersection between their wavefronts is spiral-shaped, which gives rise to a spiral intensity pattern on the camera.

from 0 to 2π by increments of $\pi/4$. With this specific antenna design, we achieved a polarization conversion of $\sim 30\%$ in power while controlling the phase of the converted beam. It is worth pointing that using phase discontinuities, one can design a single interface that achieves the effect of several beam shaping elements, which are normally cascaded along the beam path, by simply superimposing the phase response of each optical component. As an example, one can combine the cascaded effect of a vortex plate and a lens to create a focused vortex beam. To construct a phase plate that generates a single charged vortex $l=1$ (or respectively a double charged vortex $l=2$), we segment the interface in 8 (or respectively in 16) equiangular sections and each section is packed with identical antennas separated by a distance smaller than the vacuum wavelength (λ). The set of 8 (or 16) sections with incremental phase response is arranged into an azimuthal pattern, which imprints a discretized spiral phase distribution to the wavefront of the incident light. The thickness of the elements is about 60 nm which corresponds to $\sim \lambda/100$. We chose the maximum packing density of about 1 antenna per $1.5 \mu\text{m}^2$ ($\sim \lambda^2/40$) to maximize the efficiency of the device while avoiding strong near-field interactions.

Fig. 2 shows interference fringes created by the interference between a reference beam and the beam generated by the interface when the latter is incident on the camera with a small but non-zero angle relative to the first beam. In this case, interference fringes with orientation and periodicity that depend on the tilt angle are created. As shown in Fig. 2, a dislocation in the fringe pattern appears in the interferogram, confirming the presence of a phase defect at the core of the beam generated by the interface. The orientation and

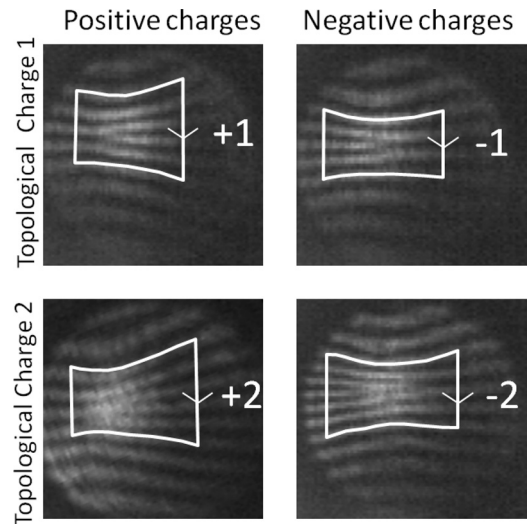


FIG. 2. Experimental results. Intensity pattern obtained from the interference between a reference beam and optical vortices with different topological charges. The dislocation of the fringe pattern indicates the presence of a phase singularity along the axis of the transmitted beam. Single (double) charge(s) vortex beams are generated by patterning the interface with an angular distribution ranging from 0 to 2π (4π). The azimuthal direction of the angular phase distribution defines the sign of the topological charge also called its chirality.

the strength of the dislocation can be used to characterize the sign and the topological charge of the vortex beam. Because the azimuthal phase profile is abruptly introduced through interaction with the antennas, the screw-like phase profile characteristic of a vortex beam can be created over a negligible propagation distance, in contrast to conventional methods (typically several millimeters for the phase addressing elements such as SLMs or the Fraunhofer distance $2D^2/\lambda$ for diffractive elements where D is the size of the element¹). Fig. 3 presents the results of a finite-domain time-difference (FDTD) simulation of a normal incident Gaussian beam ($\lambda = 7.7 \mu\text{m}$) traversing a 50×50 microns interface decorated with the same elements as the ones used in the experiments and designed to create a vortex beam with $l=1$.

To show the evolution of the vortex beam after different propagation distances, we plot the respective intensity and phase profiles of the cross polarized beam behind the interface. The amplitude becomes symmetric and reaches its final distribution when all of the partial waves from all the elements have interfered, but because the screw-like phase profile is abruptly introduced, the phase dislocation is already

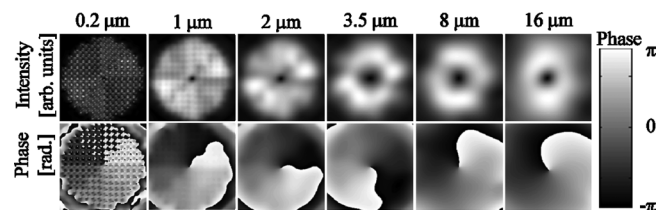


FIG. 3. FDTD simulation of a light beam that traverses an interface designed to create a single charged optical vortex. The intensity cross-sections in cross polarization with respect to the incident beam are shown at difference distances away from the interface. The characteristic zero intensity at the center of the vortex beam develops as soon as the evanescent near-field components vanish, i.e., about one wavelength behind the interface.

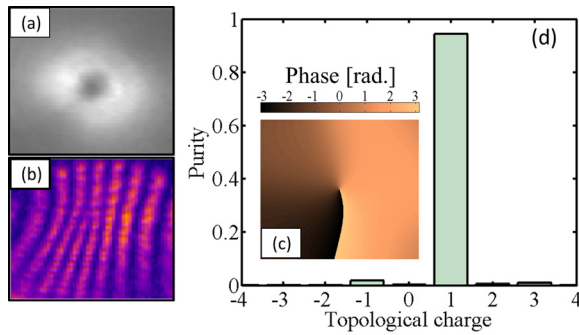


FIG. 4. (Color online) Analysis of the purity of the optical vortices based on experimental data. (a) Measured doughnut shaped intensity profile of a vortex beam. (b) Measured interferogram of the vortex beam. The phase profile of the vortex beam in (c) is extracted via 2D Fourier and inverse Fourier transforms of the interferogram in (b), separating the vortex beam and the reference beam in the Fourier space. (d) Histogram representing the decomposition of the single charged vortex beam using as the basis of LG modes with azimuthal index l_0 .

observed a micron ($\sim\lambda/8$) away from the interface. The presence of such phase singularity produces the characteristic zero of intensity at the core of the optical vortex beam less than a wavelength away from the device.

We characterized the efficiency of our device by conducting a quantitative analysis of the phase distribution of a single charged vortex beam. The amplitude distribution is obtained from the measured intensity distribution of the vortex beam (Fig. 4(a)) and the phase profile of the optical vortex is extracted from the interferogram (Fig. 4(b)). The purity of the optical vortex is calculated by decomposing its complex field on a complete basis set of optical modes with angular momentum, i.e. the Laguerre-Gaussian modes (E_{lp}^{LG}).¹⁸ The weight of a particular LG mode in the vortex beam is given by the scalar product: $C_{lp}^{LG} = \iint_{\infty} E_{vortex} \overline{E_{lp}^{LG}} dx dy$, where E_{vortex} is the vortex beam electric field, the integer p (l) is the radial (azimuthal) Laguerre-Gaussian mode index, and the upper bar denotes the complex conjugate. The relative charge distribution of an optical vortex is obtained by summing all the modes with the same azimuthal index l_0 , $C_{l_0} = \sum_p C_{p,l_0}^{LG}$. A histogram representing the relative charge distribution for our vortex beam is plotted in Fig. 4(d). The purity of the single charged vortex ($l=1$) created with our technique is above 90% which is similar to the purity of vortex beams obtained with conventional spatial light modulators, confirming the remarkable potential of these plasmonic interfaces for addressing the phase of a light beam. The ratio between the cross polarized light generated by the interface and the amount of light transmitted without interaction can easily be controlled by either changing the antenna packing density or by tailoring the scattering amplitude of each element.

In conclusion, we have proposed and demonstrated a plasmonic phased array that creates phase changes over a subwavelength propagation distance. The concept of phase discontinuity introduced in Ref. 4 opens the door to the development of ultra thin and integrated photonics devices. We envision creating reconfigurable spatial light modulators by using materials whose optical properties can be tuned by

means of external excitations.^{19,20} Finally, it should be mentioned that such interface can combine in a single ultra thin layer the effects of multiple and thick optical devices, which is promising for applications such as aberration correction and integrated optics. Reconfigurable optical phased arrays with subwavelength control of phase and amplitude could eventually lead to a technology that would challenge current liquid crystal displays.

The authors thank G. Aoust for fruitful discussions. We also acknowledge support from the National Science Foundation (NSEC) under contract NSF/PHY 06-46094, and the Center for Nanoscale Systems (CNS) at Harvard University. P.G. acknowledges funding from the Robert A. Welch Foundation (A-1261). J.L. acknowledges the fellowship support from the agency for Science, Technology and Research (A*STAR), Singapore. Z.G. acknowledges funding from the European Communities Seventh Framework Programme (FP7/2007-2013) under grant agreement PEOF-GA-2009-235860. M.A.K. is supported by the National Science Foundation through a Graduate Research Fellowship. Harvard CNS is a member of the National Nanotechnology Infrastructure Network (NNIN). The Lumerical FDTD simulations were run on the Odyssey cluster supported by the Harvard Faculty of Arts and Sciences (FAS) Sciences Division Research Computing Group. This work was supported in part by the Defense Advanced Research Projects Agency (DARPA) N/MEMS S&T Fundamentals program under grant N66001-10-1-4008 issued by the Space and Naval Warfare Systems Center Pacific (SPAWAR).

- ¹M. Born and E. Wolf, *Principles of Optics*, 7th ed. (Cambridge University Press, Cambridge, 1999).
- ²J. E. Curtis, B. A. Koss, and D. G. Grier, *Opt. Commun.* **207**, 169 (2002).
- ³M. Padgett and R. Bowman, *Nat. Photonics* **5**, 343 (2011).
- ⁴N. Yu, P. Genevet, M. A. Kats, F. Aieta, J. P. Tetienne, F. Capasso, Z. Gaburro, *Science* **334**, 333 (2011).
- ⁵J. F. Nye and M. V. Berry, *Proc. R. Soc. London A* **336**, 165 (1974).
- ⁶M. Padgett, J. Courtial, and L. Allen, *Phys. Today* **57**(5), 35 (2004).
- ⁷L. Allen, M. W. Beijersbergen, R. J. C. Spreeuw, and J. P. Woerdman, *Phys. Rev. A* **45**, 8185 (1992).
- ⁸M. W. Beijersbergen, R. P. C. Coerwinkel, M. Kristensen, and J. P. Woerdman, *Opt. Commun.* **112**, 321 (1994).
- ⁹N. R. Heckenberg, R. McDuff, C. P. Smith, and A. G. White, *Opt. Lett.* **17**, 221 (1992).
- ¹⁰V. Yu, M. V. Vassetsov, and M. S. Soskin, *JETP Lett.* **52**, 429 (1990).
- ¹¹A. G. White, C. P. Smith, N. R. Heckenberg, H. Rubinsztein-Dunlop, R. McDuff, C. O. Weiss, and C. Tamm, *J. Mod. Opt.* **38**, 2531 (1991).
- ¹²M. Berry, J. Nye, and F. Wright, *Philos. Trans. R. Soc. London* **291**, 453 (1979).
- ¹³P. Couillet, L. Gil, and F. Rocca, *Opt. Commun.* **73**, 403 (1989).
- ¹⁴P. Genevet, S. Barland, M. Giudici, and J. R. Tredicce, *Phys. Rev. Lett.* **104**, 223902 (2010).
- ¹⁵S. H. Hell, *Science* **316**, 1153 (2007).
- ¹⁶J. Leach, M. J. Padgett, S. M. Barnett, S. Franke-Arnold, and J. Courtial, *Phys. Rev. Lett.* **88**, 257901 (2002).
- ¹⁷G. Gibson, J. Courtial, M. Padgett, M. Vassetsov, V. Pas'ko, S. Barnett, and S. Franke-Arnold, *Opt. Express* **12**, 5448 (2004).
- ¹⁸A. E. Siegman, *Lasers* (University Science Books, Sausalito, CA, 1986), Chap. 16.
- ¹⁹K. F. MacDonald, Z. L. Samson, M. I. Stockman, and N. I. Zheludev, *Nat. Photonics* **3**, 2 (2009).
- ²⁰X. Wang, A. A. Belyanin, S. A. Crooker, D. M. Mittleman, and J. Kono, *Nat. Phys.* **6**, 126 (2010).